

PRUNE and NM23-M1 expression in embryonic and adult mouse brain

Pietro Carotenuto · Natascia Marino ·
Anna Maria Bello · Anna D'Angelo ·
Umberto Di Porzio · Daniela Lombardi · Massimo Zollo

Received: 20 December 2005 / Accepted: 4 January 2006 / Published online: 11 October 2006
© Springer Science+Business Media, Inc. 2006

Abstract A genetic interaction between *PRUNE* and *NM23/NDPK* has been postulated in *Drosophila melanogaster*. Many have focused on *Drosophila* for the genetic combination between *PRUNE* “knock down” and *AWD/NM23* fly mutants bearing the P97S mutation (K-pn, Killer of *PRUNE* mutation). We postulated a role for *PRUNE-NM23* interactions in vertebrate development, demonstrating a physical interaction between the human *PRUNE* and *NM23-H1* proteins, and partially characterizing their functional significance in cancer progression. Here, we present an initial analysis towards the functional characterization of the *PRUNE-NM23* interaction during mammalian embryogenesis. Our working hypothesis is that *PRUNE*, *NM23-H1* and their protein-protein interaction partners have important roles in mammalian brain development and adult brain function. Detailed expression analyses from early mouse brain development to adulthood show significant co-expression of these two genes during embryonic stages of brain development, especially focusing on the cortex, hippocampus, midbrain and cerebellum. We hypothesize that their abnor-

mal expression results in an altered pathway of activation, influencing protein complex formation and its protein partner interactions in early embryogenesis. In the adult brain, their function appears concentrated towards their enzyme activities, wherein biochemical variations can result in brain dysfunction.

Keywords PDE · cAMP · NDPK · Neurogenesis · Differentiation · Proliferation · Brain development · *PRUNE* · *NM23*

Introduction

A potential genetic interaction between *PRUNE* and *NM23/NDPK* has been postulated since the studies performed in *Drosophila melanogaster* in the early 1960s. The *abnormal wing discs (AWD)* gene identified in *Drosophila* (Dearolf et al., 1988a,b) encodes a protein that is 78% identical to human *NM23* (also known as *NM23-H1*) (Rosengard et al., 1989). At the same time, the *PRUNE* gene was identified from viable mutations that cause a brownish-purple eye color phenotype. The *PRUNE* gene encodes a single 1.8 kb transcript that is predicted to be translated into a 44.5 kDa protein (Frolov et al., 1994).

The genetic combination between these two genes and their protein functions was originally shown by the lethal interaction between the *AWD^{Kpn}* mutation and *PRUNE* (Sturtevant, 1956). The *AWD^{Kpn}* mutation (also known as the *Killer of Prune (Kpn)* mutation) in *Drosophila* is a point mutation in the *AWD* gene that results in a substitution of proline at position 97 for serine (Biggs et al., 1988; Lascu et al., 1992). In the absence of a functional *PRUNE* gene product, the *AWD^{Kpn}* mutation is lethal (Timmons et al., 1995); double mutants die at the second or third larval

P. Carotenuto · N. Marino · A. M. Bello · A. D'Angelo · M. Zollo
CEINGE, Biotecnologie Avanzate Scarl, Via Comunale
Margherita 482, 80145 Naples, Italy

M. Zollo (✉)
Dipartimento di Biochimica e Biotecnologie Mediche,
Università degli Studi di Napoli “Federico II”
via Pansini 5, Naples, Italy
e-mail: zollo@ceinge.unina.it

U. di Porzio
IGB, Institute of Genetics and Biophysics “Adriano
Buzzati-Traverso,” CNR, Naples, Italy

D. Lombardi
Department of Experimental Medicine, University of L'Aquila,
L'Aquila, Italy

instar stage as they acquire a melanotic phenotype in swelling cells taking part in imaginal disc structures that do not follow normal tissue development (Timmons et al., 1996). Additionally, gynandromorph mosaic experiments have suggested that the *PRUNE*/*AWD*^{K^{pn}} focus lethality corresponds to a region from which the mesodermal and nervous systems develop (Orevi and Falk, 1974). By cytology experiments, a considerable hypertrophy of the neuroglia and the perineurium of the larval brain has been described (Hackstein, 1992). Furthermore, the genetic combination of *PRUNE* and *AWD*/*NDPK* in *Drosophila* constitutes a highly specialized genetic system with intriguing implications in vertebrate development and oncogenesis.

The *AWD*/*NDPK* human homolog, *NM23-H1*, was isolated on the basis of its reduced expression in highly metastatic murine melanoma cell lines, as compared with their non-metastatic counterparts (Steege et al., 1988). The anti-metastatic function of *NM23* was measured *in vitro* and *in vivo*, demonstrating effects on motility and invasion, with its involvement established in breast, melanomas (Leone et al., 1991, 1993) and prostate carcinomas (Lim et al., 1998), and most likely in colon carcinomas (Suzuki et al., 2004). In human, eight genes (*NM23-H1* to *NM23-H8*) have been described, and NDPK activities have been shown in only six of these eight gene members isolated (Lacombe et al., 2000).

We identified the human *PRUNE* protein, showing that it physically interacts with human *NM23-H1* and with *NM23-H1* carrying a “K^{pn} mutation” (P96S), but not with *NM23-H1-SI20G*, a gain-of-function mutation associated with advanced neuroblastoma stages (Reymond et al., 1999; Forus et al., 2001). Additionally, we characterized the *PRUNE* enzyme activity, showing that it has the phosphodiesterase (PDE)-cAMP activity of the DHH family of proteins, and that this *PRUNE* PDE-cAMP activity is enhanced by its interaction with *NM23-H1*, thus stimulating cellular motility and metastasis processes (D’Angelo et al., 2004). While the formation of the *PRUNE*-*NM23* complex during tumor development and progression has begun to be deciphered (Garzia et al., 2005, in preparation), at present, the hypothesis of coordination between the two proteins during development is supported only by the demonstration that both of these proteins are a part of the same genetic pathway in *Drosophila*.

Several observations have suggested the involvement of the *NM23* genes in the development of a variety of cellular functions related to embryogenesis, including roles in cell proliferation, migration, differentiation and apoptosis (Lombardi et al., 2000; Amendola et al., 2001; Otero et al., 2000). The molecular mechanisms underlying the role of *NM23-H1* in development do not appear to be associated with its NDPK activity, and to date, this additional function and its mechanism of action remain under inves-

tigation. The pattern of expression of the mouse homolog *NM23-M1* has been studied during mouse embryogenesis and organogenesis; the *NM23-M1* transcript was shown to be widely distributed throughout the embryonic and adult mouse central nervous system (CNS), with prominent expression in several restricted areas (Dabernat et al., 1998, 1999; Gervasi et al., 1998; Lakso et al., 1992; Amrein et al., 2005).

The hypothesis of an important role for *NM23-H1* in CNS development is supported by evidence of the involvement of *NM23-H1* in neuronal differentiation and migration, as shown in model cell systems. Using a neuronal differentiation model system, rat pheochromocytoma PC12 cells, overexpression of *NM23-M1* was seen to enhance NGF-induced sympathetic neuronal cell differentiation by influencing cell proliferation and neurite outgrowth (Gervasi et al., 1996). In addition, *DR-nm23* (the *NM23-H3* gene) promotes differentiation of neuroblastoma cells towards neuronal and schwannocytic phenotypes, and induces changes in the adhesion properties of those cells due to a modulation of their pattern of integrin expression (Amendola et al., 1997). Furthermore, in rat C6 glioma cells, the rat homolog of *NM23-M1*, *NM23-R1*, was seen to be up-regulated upon cAMP-induced differentiation, and associated with the intermediate filament proteins, *GFAP* and *vimentin* (Roymans et al., 2000). However, to date, the mechanisms underlying the role of *NM23-H1* in neural differentiation still remain unclear and poorly understood.

Two main questions have been raised at this stage: (1) Are the *PRUNE* and *NM23* proteins expressed at the same time during brain development? (2) Can *PRUNE* control *NM23* function in mouse brain development?

To address the question of *PRUNE* and *NM23-M1* functions in brain development, we started a comprehensive gene expression analysis in embryonic and adult mouse brain, focusing our attention on co-expression of these two genes in several CNS-specific compartments and tissues during mouse development. We thus hypothesized that *PRUNE* regulates *NM23* functions following two main features: (a) in *Drosophila*, genetic interactions between *PRUNE* and *AWD*/*NM23* influence larval brain development; (b) the protein-protein interactions between *PRUNE* and *NM23* in human provide a negative regulation of the anti-motility effects of *NM23-H1*, thus leading to breast cancer metastasis (D’Angelo et al., 2004).

Materials and methods

Tissue preparation

All of the studies were conducted in accordance with the principles and procedures outlined in the National Institutes

of Health Guidelines for Care and Use of Experimental Animals. Fresh-frozen, post-fixed sections were used for all of the experiments. At least one litter for each age group from which data are reported (E10.5, E12.5, E14.5, E16.5 and P0) was used, with at least two embryos examined at each age. Pregnant CD1 mice were decapitated. For embryos of E10.5, E12.5 and E14.5, the whole uteri were freshly frozen and embedded in OCT compound for cryostat sectioning. Mouse embryos older than E14.5 were dissected quickly and staged according to their limb-bud morphology using the criteria described previously (Wanek et al., 1989) before being frozen and embedded in OCT. Embryonic trunk sagittal and transverse sections (14 μ m) were prepared to detail the expression patterns. Sections were mounted onto 3-aminopropyltriethoxy-silane-coated microscope slides and stored at -80°C until their use in the hybridization procedures.

Probes

Digoxigenin-labeled RNA probes for mouse *PRUNE* (named *PRUNE-MI*) (NM_173347) and *NM23-MI* (NM_008704) were synthesized and purified *in vitro* from the plasmid vectors harboring the appropriate cDNA sequences. For *PRUNE*, an 853 bp PCR fragment that was generated from T7 and SP6 primers corresponding to nt 198 to 998 of the mouse *PRUNE* was transcribed with SP6 RNA polymerase to make the antisense probe. For *NM23-MI*, a 633 bp PCR fragment that was generated from T7 and SP6 primers corresponding to nt 100 to 733 of the mouse *NM23-MI* was transcribed with SP6 RNA polymerase to make the antisense probe. To produce sense probes, we transcribed PCR fragments with T7 RNA polymerase. The digoxigenin-labeled RNA probes were prepared with the DIG RNA Labeling Kit from Roche, according to the protocol supplied.

In situ hybridisation

Digoxigenin-labeled hybridisations were carried out on tissue sections as described previously (Bovolenta et al., 1997). Briefly, the embryos were fixed in 4% paraformaldehyde in 0.1 M phosphate buffer (PB; pH 7.3) at 4°C overnight, and then cryoprotected by immersion in 30% sucrose solution in PB. Cryostat sections (14 μ m) were mounted on 3 aminopropyltriethoxy-silane-coated slides and air dried. After rinses in phosphate-buffered saline (PBS), the sections were prehybridised for 1 h at 60°C in 50% formamide buffer, incubated with digoxigenin probes for 16 h at 60°C , and further washed at the same temperature. After incubation in 2% Roche blocking reagent solution for 1 h, the sections were incubated with an AP-coupled antidigoxigenin antibody (Roche), diluted 1:2000. The slides were

transferred to coplin jars and washed 3×5 min in MABT, and then 2×10 min in prestaining buffer (100 mM Tris-HCl, pH 9, 100 mM NaCl, 5 mM MgCl_2). The prestaining buffer was replaced with staining buffer (100 mM Tris-HCl, pH 9, 100 mM NaCl, 5 mM MgCl_2 , 5% [w/v] polyvinyl alcohol [mean MW 70–100 kDa, Sigma], 0.2 mM 5-bromo-4-chloro-3-indolyl-phosphate [BCIP, Boehringer], and 0.2 mM nitroblue tetrazolium salt [NBT, Boehringer]), and incubated in the dark at room temperature until the signal reached a satisfactory intensity (usually a few hours to overnight, although, exceptionally, over a weekend). The slides were then washed in distilled water for 30 min, dehydrated through ascending ethanol concentrations (30%, 60%, 80%, 95% and 100%, for 1 min each), cleared in xylene, mounted under cover slips in XAM mountant (BDH), and analysed under a Leica DC500 compound microscope.

Immunohistochemistry

Mouse brain sections were rinsed in 100 mM Tris buffered saline, pH 7.4 (TBS), and blocked in TBS containing 0.1% Triton X-100 and 5% goat serum (GS) for 1 to 2 h at room temperature. The tissue sections were incubated with affinity purified antibodies in TBS containing 0.1% Triton X-100 and 2.5% GS overnight at $4-8^{\circ}\text{C}$. The specific antibodies used in this study were anti-*PRUNE* (polyclonal A59, generated in rabbit, and monoclonal 2/C32 generated in mouse—Alexis) antibodies raised in GS (1:100 dilution), an anti-*NM23* (polyclonal K73—Alexis) antibody generated in rabbit (1:100 dilution), an anti-tyrosine hydroxylase (1–300 dilution—monoclonal—Babco), an anti-TUJ1 (1–500 dilution—monoclonal—Babco). Following four washes with TBS containing 0.5% Tween 20 (TBST) of 15 min each, the tissue sections were incubated for 2 h at room temperature with TRITC at a 1:200 dilution, or with FITC conjugated at a 1:200 dilution in TBS containing 0.1% Triton X-100 and 2.5% GS. The tissue sections were washed four times in TBST over 2 h, placed in 100 mM Tris (pH 7.4) and mounted on microscope slides. Following a brief rinse with water, the sections were allowed to air dry for at least 1 h. The fluorescent immunocomplexes were detected using a Axion microscope Zeiss. The channel sensitivity was optimized for each set of stained sections, and then maintained for that group of samples. Typical sensitivity settings ranged from 1.5 to 3.0.

Results

Non radioactive *in situ* hybridization was used to evaluate the mRNA expression patterns of mouse *PRUNE* gene (also named) *PRUNE-MI* and *NM23-MI* during development of

the mouse brain from E10.5 to adulthood. Serial sagittal and coronal sections were hybridized with antisense and sense probes of *PRUNE-M1* and *NM23-M1*. The control sections hybridized with sense probes did not show specific staining (data not shown). In addition, an immunohistochemical analysis was performed to reveal the protein expression patterns. A description of the expression of *PRUNE-M1* and *NM23-M1* in different brain areas in mouse development is given below.

Cortex

At embryonic day E10.5, which corresponds to the early stages of telencephalic development, the two genes show complementary patterns of expression. The expression in telencephalic vesicles is very high both for *PRUNE-M1* and for *NM23-M1*, as shown by expression analyses on whole-mount embryos (Fig. 1A, D) and on parallel sagittal and coronal sections at E10.5 (Fig. 1B, C, E, F). At E14.5,

the two mRNAs were detected in the neopallial cortex in many densely packed cells (Fig. 2A, B) and in all layers of the developing telencephalon (Fig. 2C–F). A strong expression of *PRUNE-M1* and *NM23-M1* transcripts in all of the cell bodies forming the cortical developing layers was seen (Fig. 2E, F). Interestingly, the immunohistochemical analysis of the coronal sections at E14.5 revealed a different expression pattern of these two proteins: here, *PRUNE-M1* is preferentially expressed in the ventricular zone (Fig. 2G), while *NM23-M1* is more highly expressed in the layers of the forebrain mantle of the developing telencephalon (Fig. 2H). After birth, *PRUNE-M1* and *NM23-M1* mRNA expressing cells are present in the cortex, where they assume a more sharp and defined pattern following the progressive organization of the different cortical layers. At postnatal days P0 (Fig. 3) and P5 (data not shown), the strongest *PRUNE-M1* and *NM23-M1* staining was seen in developing layers 2–4 and in the subplate layer, while a more weak expression at the mRNA level was detected in the ventricular zone

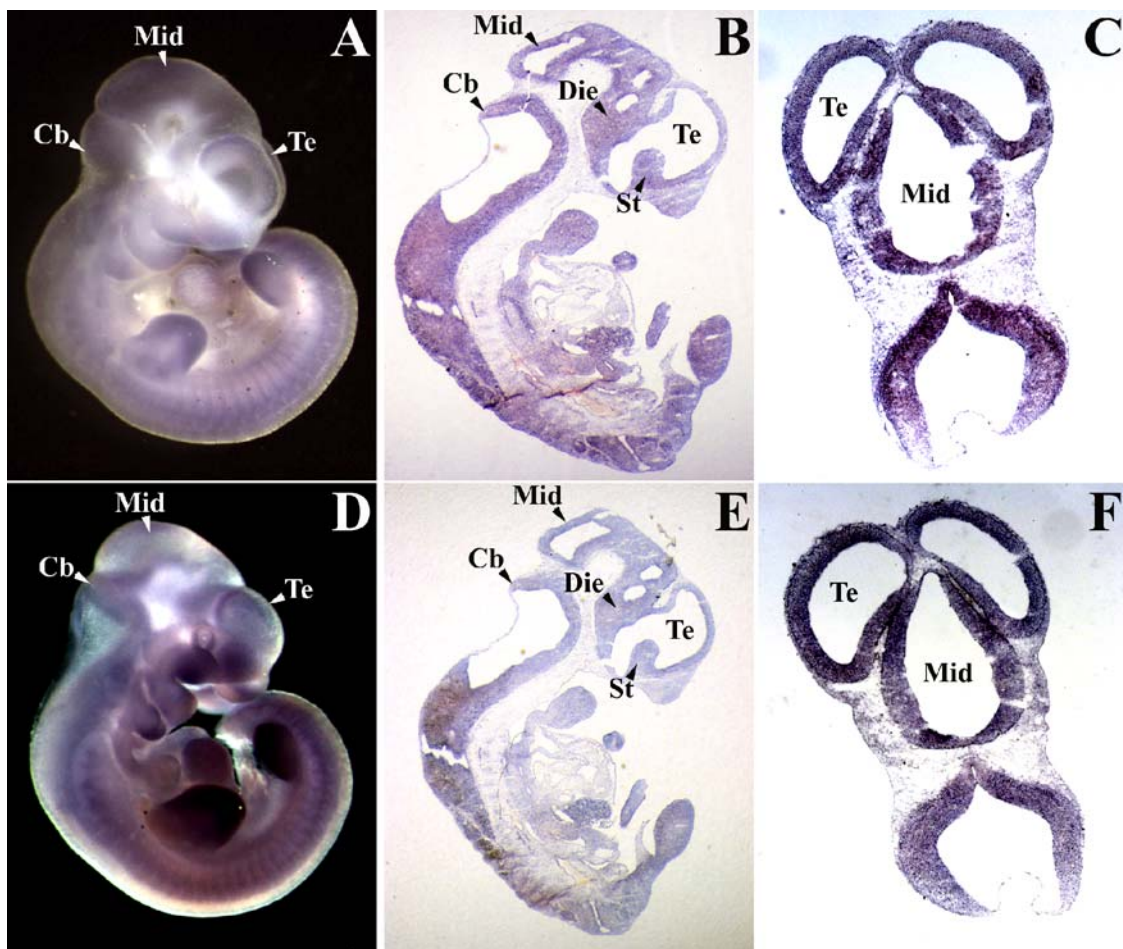
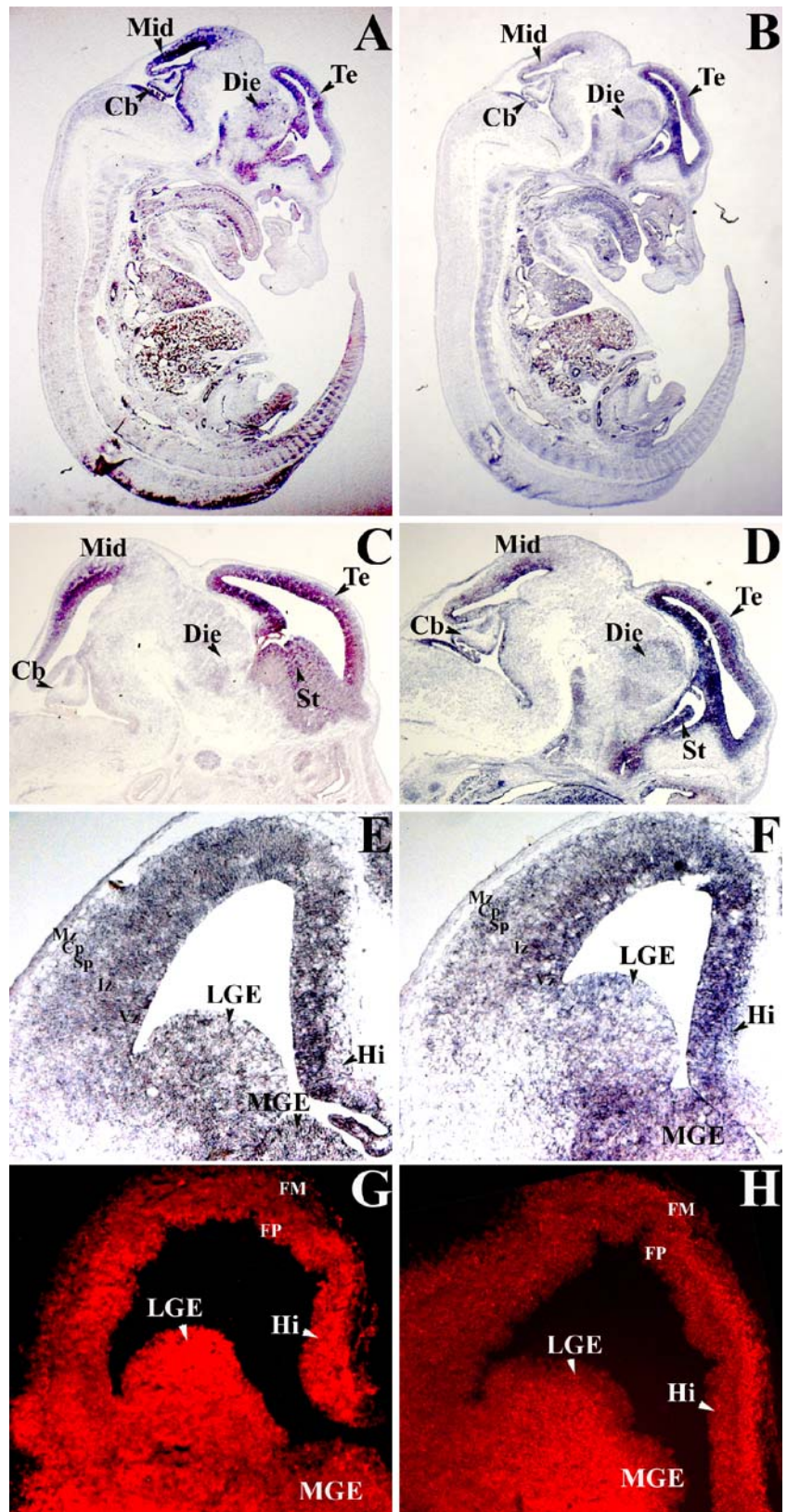


Fig. 1 Expression analysis of *PRUNE-M1* and *NM23-M1* at embryonic day E10.5. Detection of *PRUNE-M1* (A–C) and *NM23-M1* (D–F) expression by *in situ* hybridization on whole mount E10.5 mouse embryos (A, D) and sagittal (B, E) and coronal (C, F) sections using

digoxigenin-labeled antisense riboprobes. The mRNAs are seen in the developing telencephalon (Te), the midbrain (Mid), the cerebellum primordium (Cb), the diencephalon (Die) and the striatum primordium (St). Scale bars = 200 μm

Fig. 2 Expression analysis of *PRUNE-M1* and *NM23-M1* at embryonic day E14.5. Photomicrographs showing the distribution of the *PRUNE-M1* (A, C, E) and *NM23-M1* (B, D, F) mRNAs in sagittal (A–D) and coronal (E, F) sections of mouse embryo at E14.5 by *in situ* hybridization with digoxigenin-labeled probes. The *PRUNE-M1* and *NM23-M1* transcripts are seen at high levels of expression in the developing telencephalon (Te), hippocampus (Hi), striatum (St), diencephalon (Die), midbrain (Mid) and cerebellum primordium (Cb) (A–D). At E14.5, all of the layers of the developing telencephalon (Mz, marginal zone; Cp, cortical plate; SP, subplate; Iz, intermediated zone; Vz, ventricular zone) display high levels of *PRUNE-M1* and *NM23-M1* mRNAs (E, F). Coronal sections of mouse telencephalon at E14.5 were stained with antibodies against *PRUNE* (G) and *NM23* (H). Each antibody was visualized with a TRITC-conjugated secondary antibody (red). The *PRUNE* and *NM23* proteins were detected in the developing forebrain mantle (FM), in the proliferative forebrain (FP), in the hippocampus (Hi) and in the lateral and medial ganglionic eminence (LGE, MGE). Scale bars = (A–D) 1 mm; (E–H) 50 μ m



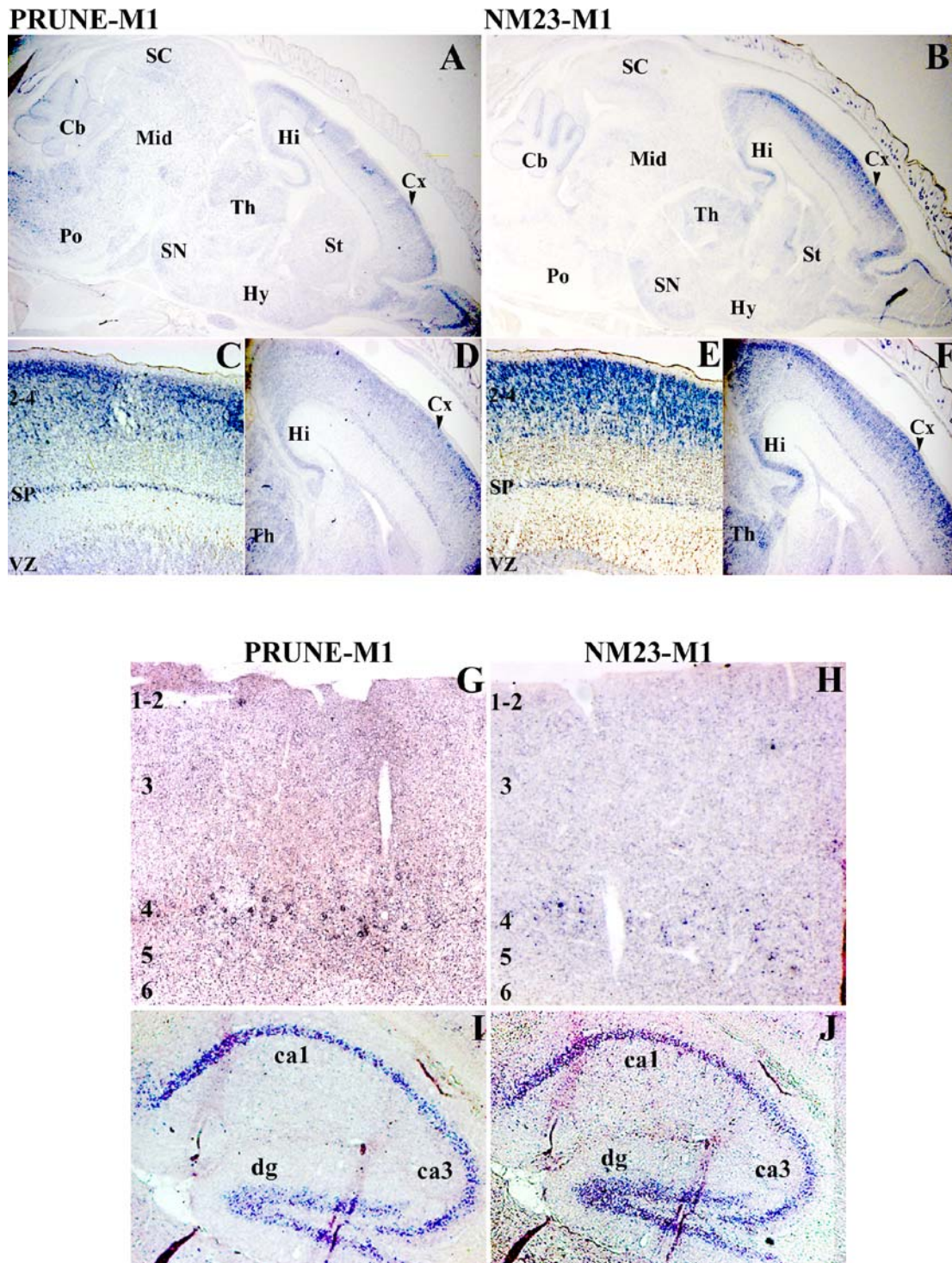
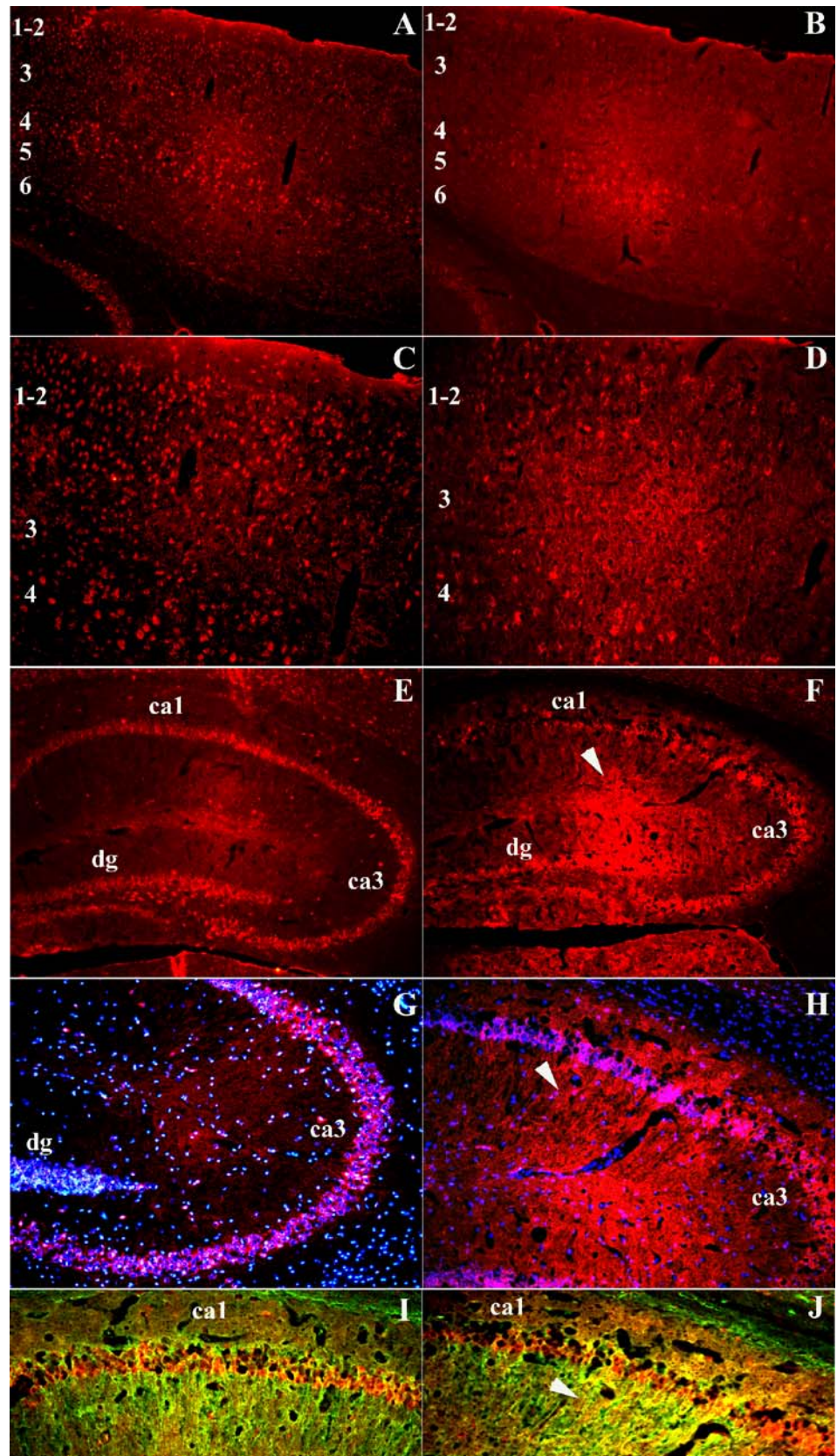


Fig. 3 Expression patterns of the *PRUNE-M1* and *NM23-M1* transcripts in mouse brain, at postnatal day P0 and in the adult. Expression patterns of *PRUNE-M1* (A, C, D) and *NM23-M1* (B, E, F) mRNAs, as detected by *in situ* hybridization, at post-natal day P0 in mouse brain. Preferential expression is seen in the cortex (Cx), the striatum (St), the hippocampus (Hi), the thalamus (Th), the hypothalamus (Hy), the substantia nigra (SN), the midbrain (Mid), the superior colliculus (SC), the cerebellum (Cb) and the pons (Po). In the cortex, the two transcripts

have a strong expression in layers 2–4 in the subplate (SP) and in the ventricular zone (VZ). In adult brain (G–J), *PRUNE-M1* mRNA expression (G, I) was detected in layers 1–2 and 4 of the cerebral cortex (G), and in ca1, ca3 and the dentate gyrus area (dg) of the hippocampus (I). *NM23-M1* mRNA expression (H, J) is lower and more widely spread in layer 1–2, and higher in layer 4 of the cerebral cortex (H), and is detected in ca1, ca3 and the dentate gyrus area (dg) of the hippocampus (J). Scale bars = (A, B) 1 mm; (C–J) 50 μ m

Fig. 4 Localization of the PRUNE and NM23 proteins in adult mouse cortex and hippocampus. Cerebral cortex sagittal sections (A–F) stained with an anti-*PRUNE* antibody (A, C, E; red) show weak staining of layers 1-2 and 4 of the adult brain cortex (A, detail in C), and of ca1, ca3 and the dentate gyrus regions of the hippocampus (E). Staining with an anti-*NM23* antibody (B, D, F; red) shows weak staining of layers 1-2 and 4 of the adult brain cortex (B, detail in D), and of ca1, ca3 and the dentate gyrus regions of the hippocampus (F). The white arrow in F shows the expression of *NM23* in dentate gyrus (dg) neuron processes. The high magnification photomicrographs (G–J) show the ca3 region of the adult hippocampus (G, H) immuno-stained with either an anti-*PRUNE* antibody (G; red) or an anti-*NM23* antibody (H, red), both with DAPI staining (blue). These also show the ca1 region double-stained with either anti-*PRUNE* (red) and anti-*TUJ1* (green) antibodies (I), or with anti-*NM23* (red) and anti-*TUJ1* (green) antibodies (J). White arrows indicate the *NM23* protein expression spreading into the projection of the neurons into the molecular layer of the dentate gyrus (dg). Scale bars = (A–F) 100 μ m; (G–J) 200 μ m



(Fig. 3C–F). In the adult forebrain, *PRUNE-M1* and *NM23-M1* mRNA expression was observed in the cell bodies, with variable intensities throughout the different cortical layers, although the strongest labeled signal was observed in layers 1–2 and 4 for *PRUNE-M1* (Fig. 3G). *NM23-M1* mRNA was detected in layer 4 and in all layers of the adult cortex, although with a lower intensity (Fig. 3H). Generally, *PRUNE-M1* retains a stronger and wider expression in the adult cortical layers than *NM23-M1*. The immunohistochemical staining with anti-*PRUNE* and anti-*NM23* antibodies showed expression patterns that are complementary to the *in situ* mRNA analyses. As shown in Fig. 4, the *PRUNE* protein is abundant and highly expressed in neurons of cortical layers 1–2 and 4 of the adult mouse cortex (Fig. 4A, C), while the *NM23* protein is seen in layer 4 (Fig. 4B, D). In the adult cortex, the *NM23* protein expression pattern is low and well defined (Fig. 4B, D), while that of the *PRUNE* protein shows a wide expression in all of the layers of the cortex, with preferential, and strong, expression in layers 2 and 4 (Fig. 4A, C).

Basal forebrain and striatum

During development of the basal brain and striatum, the *PRUNE-M1* and *NM23-M1* mRNAs were strongly expressed after E10.5 in the primordium of the subpallium region (Fig. 1B, E). At E14.5, the expression of the two mRNAs remained high in the whole striatum, both in the medial and the lateral ganglionic eminences (Fig. 2C–F). The expression in the striatum was confirmed at the protein level by immunohistochemical staining (Fig. 2G, H). During development, the intensity of the labeling signals in the corpus striatum becomes lower, although the expression of *PRUNE-M1* and *NM23-M1* was detected in all of the nuclei forming striatum at P0, such as in the caudate putamen and globus pallidus (Fig. 3A, B). In the adult, the basal forebrain area does not show any striking signals at either the mRNA or the protein level (data not shown).

Hippocampus

In the hippocampal area, both *PRUNE-M1* and *NM23-M1* mRNAs were seen to be highly expressed during development at the E10.5 (Fig. 1) and E14.5 (Fig. 2) stages. After birth, at P0, the two transcripts were present in the pyramidal cells of the CA1–CA3 region and in the granule cells of the dentate gyrus (Fig. 3C, F). The same mRNA expression pattern was observed in the adult hippocampus (Fig. 3I, J). To better define these expression patterns of *PRUNE-M1* and *NM23-M1*, we investigated their protein levels and their patterns and neuron specification in the adult brain sections by double labeling using a neuronal marker

(an anti-*TUJ1* antibody). In the adult mouse hippocampus, *PRUNE-M1* and *NM23-M1* co-localize with *TUJ1* predominantly in the cell bodies of the CA1–CA3 region and into the dentate gyrus (Fig. 4E–J). Interestingly, the *NM23* protein expression spreads into the projection of the neurons into the molecular layer of the dentate gyrus (see arrows in Fig. 4F, H, J).

Thalamus and hypothalamus

At E10.5, the *PRUNE-M1* and *NM23-M1* mRNAs were detected in the developing diencephalon (Fig. 1). Strong expression was seen at E14.5 in the entire developing epithalamic and hypothalamic areas (Fig. 2). From P0 to adulthood, the expression levels of these two transcripts were found to be low and hardly detectable in the thalamus and the hypothalamus. Specifically, at P0, *PRUNE-M1* was widely expressed in the entire thalamus and hypothalamus, whereas the *NM23-M1* levels of expression were higher in the epithalamus and the ventral thalamus than in the hypothalamus (Fig. 3A, B).

Midbrain

PRUNE-M1 and *NM23-M1* mRNA expression was high from E10.5 in the roof of the midbrain (Fig. 1B, C, E, F). At E14.5, the expression levels of these two transcripts remained very strong in the lateral developing midbrain, while in the developing tegmental area their expression was lower (Fig. 2). After birth, at P0, the *PRUNE-M1* transcript was widely expressed both in the tegmentum and the tectum areas, whereas the *NM23-M1* mRNA was hardly detectable in the entire midbrain, except for some labeled neurons of the superior colliculus. A strong expression of the *PRUNE* and *NM23* proteins was found in the substantia nigra (Fig. 7A, B), in immunohistochemical analyses. Of note, a clear co-localization of the two proteins is observed (Fig. 7C). To better define their co-expression and to investigate in which neuron types the two genes are expressed, adult brain sections were double labeled with a specific dopaminergic neuronal marker (tyrosine hydroxylase, TH). In the substantia nigra, *PRUNE-M1* co-localizes with tyrosine hydroxylase, but interestingly, we note that not all of the neurons in this area are double labeled (see arrows in Fig. 7D–F).

Cerebellum

In the hindbrain at the early stages of the development of the cerebellum (at E10.5), the *PRUNE* and *NM23-M1* transcripts were strongly and widely expressed in the rhombic lips of the cranial edge of the thinned roof of the fourth ventricle (Fig. 1B, C, E, F). Co-expression of the two genes was observed both in the rhombic lip, from where the

precursors of granule neurons arise, and in the ventricular zone, where Purkinje cells begin their development (Fig. 5A, B). From E13.5 to E14.5, when the Purkinje neurons become differentiated, all of the compartments of the developing cerebellum were significantly labeled for both of the genes (see arrows in Fig. 5C–F). At postnatal day P0, when the external granular layer neurons begin their differentiation, we noted the strong expression of the *PRUNE* and *NM23-M1* mRNAs in their cell bodies. The *PRUNE-M1* transcript showed higher levels than that of *NM23-M1* in Purkinje cells migrating to the cerebellar surface. Generally, the levels of expression of *NM23-M1* were restricted to the external granular layer and the developing Purkinje layers, while the *PRUNE-M1* transcript was widely expressed in the entire cerebellum at P0 (Fig. 5G, H). In the adult mouse cerebellum, *PRUNE-M1* mRNA was at high levels in the Purkinje cell layer, in the internal granular layer, and in the interneurons of the molecular layer; in contrast, *NM23-M1* mRNA expression displayed a low signal that was restricted to only the molecular layer (Fig. 6A–F). Immunostaining with a Purkinje-cell-specific marker (an anti-*calbindin* antibody) revealed specific expression of the *PRUNE* and *NM23* proteins in the adult cerebellum layer (Fig. 7G–I, M–N). These data were supported by the double staining with an anti-*TUJ1* monoclonal antibody, revealing the expression of the *PRUNE* protein not only in the Purkinje cells, but also in the molecular layer and into the internal granular layer (Fig. 7J–L).

Discussion

The aim of this study was to determine if *PRUNE* and *NM23-H1* retain patterns of co-expression in various compartments of the developing mouse brain, thus postulating a controlling role for these two proteins in brain development. To do so, we analyzed the expression patterns of *PRUNE* and *NM23-M1* in embryonic and adult mouse brain at the mRNA and protein levels.

During mouse brain development, the expression of both *PRUNE-M1* and *NM23-M1* was highly evident at the early stages of organogenesis, which corresponds to the differentiation of several areas of the developing nervous system (Figs. 1 and 2). This indeed indicates a potential combined role of these two genes in the mechanisms regulating brain development. After birth, their expression is restricted to some defined brain regions that have several functional roles.

The *PRUNE-M1* and *NM23-M1* transcripts were first detected at embryonic day E10.5, when the first embryonic tissues begin to differentiate; at this stage, organogenesis is taking place, but it is still incomplete. The same expression pattern has been described for the other *NM23* isoforms (Amrein et al., 2005). Thus the *PRUNE* and *NM23s* genes

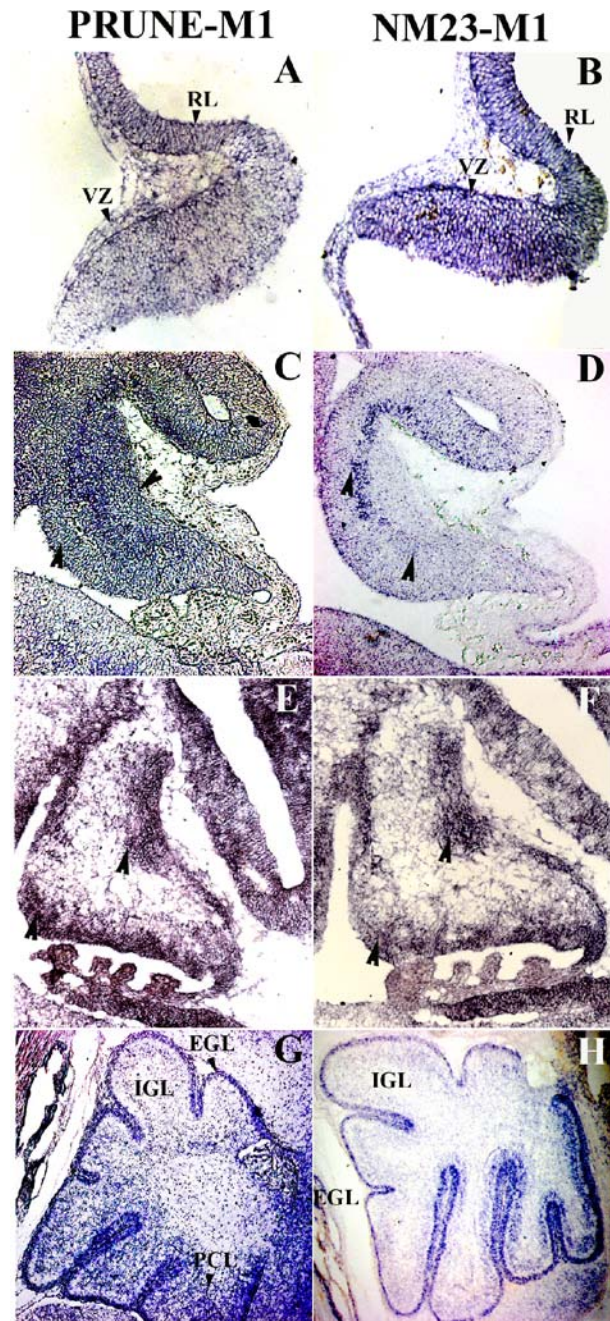
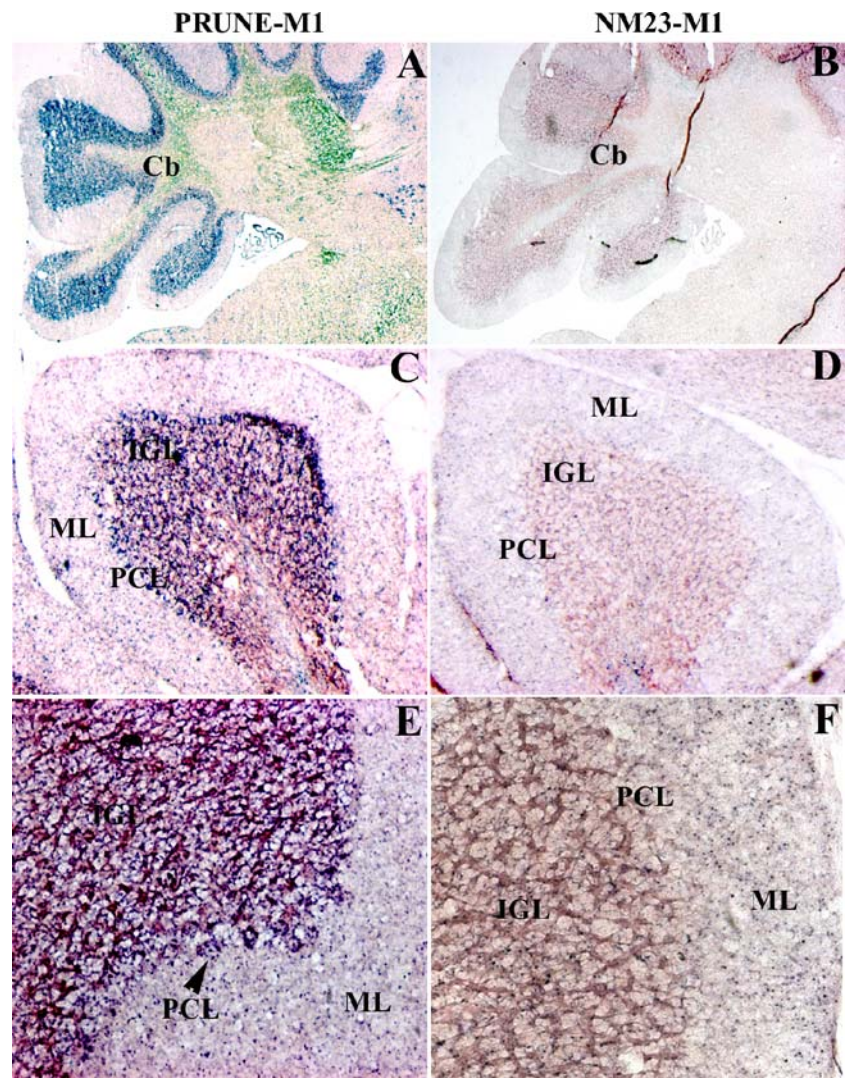


Fig. 5 Analysis of *PRUNE-M1* and *NM23-M1* expression during cerebellum development. The expression patterns of *PRUNE-M1* (A, C, E, G) and *NM23-M1* (B, D, F, H) show that both transcripts are found in the cerebellar primordium at E10.5 (A, B), E13.5 (C, D) and E14.5 (E, F). At P0 (G, H), *PRUNE-M1* mRNA is expressed in all of the layers of the cerebellum (G.), while *NM23-M1* mRNA is detected only in the external granular layer (EGL; H). PCL, Purkinje cell layer; IGL, inner granular layer. Black arrows show the highest signals in developing cerebellum at E13.5 (C, D) and E14.5 (E, F). Scale bars = (A, B) 200 μm ; (C–F) 100 μm ; (G, H) 50 μm

Fig. 6 Analysis of *PRUNE-M1* and *NM23-M1* expression in the adult cerebellum. Detection of the *PRUNE-M1* (A, C, E) and *NM23-M1* (B, D, F) expression by *in situ* hybridization on adult brain sagittal sections, using digoxigenin-labeled antisense riboprobes. *PRUNE-M1* mRNA expression is seen in all three layers of the adult cerebellum, while that for *NM23-M1* mRNA is only in the molecular layer (ML). The black arrow in E shows the high expression of *PRUNE-M1* in the Purkinje cell layer (PCL). IGL, inner granular layer. Scale bars = (A, B) 1 mm; (C, D) 50 μ m; (E, F) 200 μ m

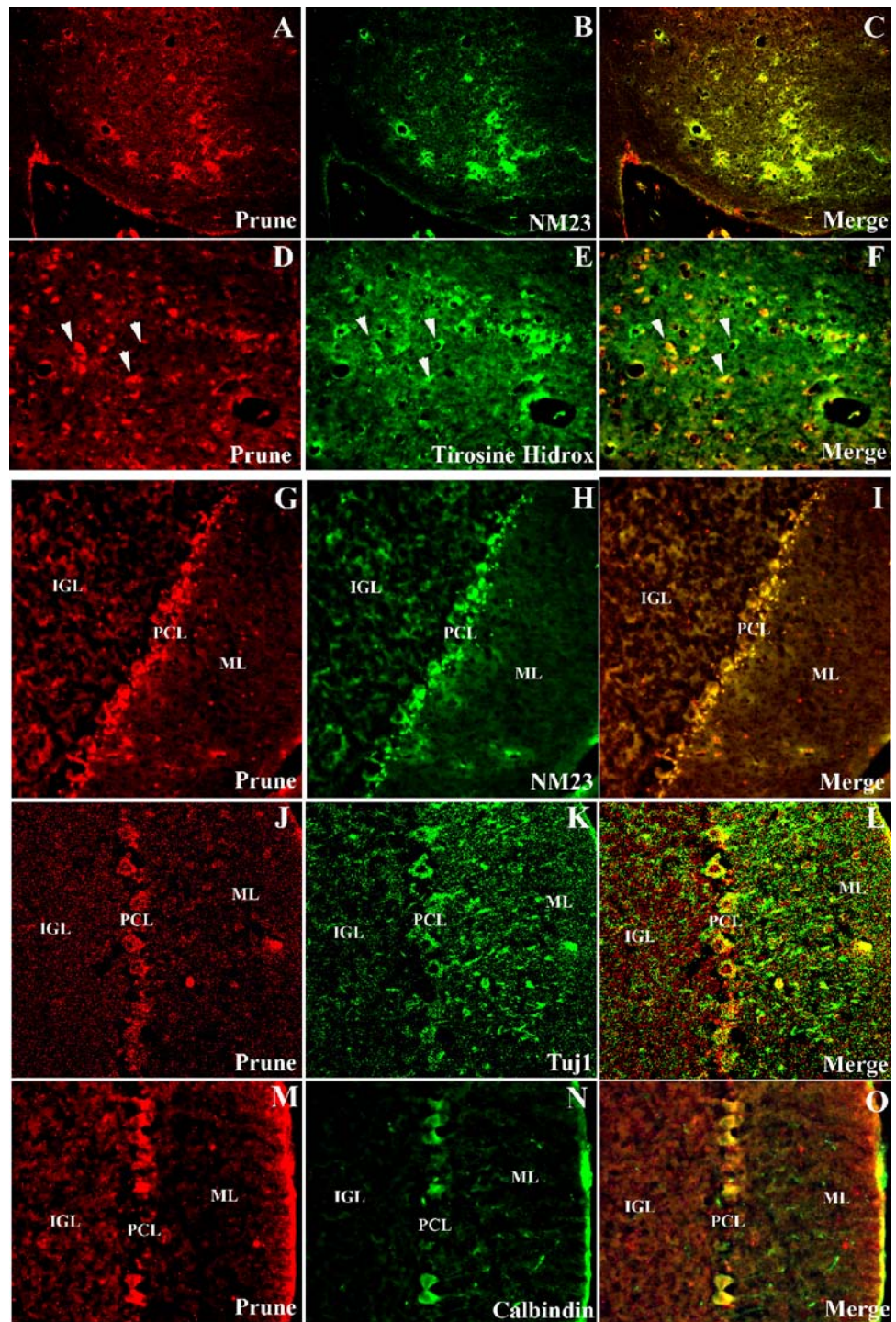


may be involved in different cellular processes and exhibit specific properties that are related to the nucleotide channeling, transcription or transduction pathways, as first described by Mesnildrey et al. (1998). Similar specificities have been suggested for other gene families that show expression patterns similar to these of the *PRUNE* and *NM23* genes, including the members of the *transforming growth factor* (*TGF- β*) gene family and their receptors (Feijen et al., 1994) and the *fibroblast growth factor* (*FGF*) gene family (Colvin et al., 1999). It is known that the *NM23* genes might be involved in the responsiveness of cells to *TGF- β* stimuli, as has been shown for many tumors (Hsu et al., 1994; Leone et al., 1991). Thus, we do not exclude the additional involvement of *PRUNE* in this signaling pathway, particularly because of its potential function on epithelial-mesenchymal transition (EMT) that have already been demonstrated for *gelsolin* and additional *PRUNE* partners in a breast cancer model (Garzia et al., in this issue), and in regulating brain development and morphogenesis. Furthermore, recent studies

on the *EBNA-3C* (Subramanian et al., 2001), *menin* (Ohkura et al., 2001) and *RORa/RZRb* (Paravicini et al., 1996) genes have suggested that the *NM23* proteins are involved in the regulation of gene transcription through specific interactions between these proteins. It is also possible that *PRUNE* participates with the *NM23* genes in the regulation of the coordinate actions of transcription factors involved in brain development at these stages of embryogenesis, although these observations need further supporting data.

At embryonic day E14.5, the *PRUNE-M1* and *NM23-M1* transcripts were strongly expressed in several areas where biological processes are taking place, such as neuronal proliferation, migration and differentiation. In particular, in the telencephalon at E14.5 the expression of both of these genes was detected in the ventricular zone of the neopallial cortex; at this stage, this area is devoted to neuron proliferation. Additionally, these genes are expressed both in the intermediate zone of the developing layer and in the ganglionic eminences, where neurons migrate to the pial

Fig. 7 Analysis of the *PRUNE-M1* and *NM23-M1* proteins expression in the adult substantia nigra and in cerebellum. Cerebral sagittal sections (A–F) stained with an anti-*PRUNE* antibody (A, detail in D; C, detail in F; red) and either anti-*NM23* (B, C; green) or anti-tyrosine hydroxylase (detail in E, F; green) antibodies show the overlapping staining of the substantia nigra neurons. The yellow signal in C, F shows the merge of each of the two staining patterns. The adult cerebellum layers (G–O) immunostained with an anti-*PRUNE* antibody (G, J, M; red) and either anti-*NM23* (H; green), anti-*TUJ1* (K; green) or anti-*calbindin* (N; green) antibodies show co-expression of all of these protein pairs in the Purkinje cell layer (PCL; yellow merge signals in I, L, O, respectively), and of *PRUNE* and *NM23* in the molecular layer (ML; I) and of *PRUNE* and *Tuj1* in neuron processes of the ML (L). IGL, inner granular layer. White arrows show respectively labeled neurons positive to anti-*PRUNE* antibody (red) in substantia nigra (D), to anti-Tyrosine Hydroxylase (green) (E), and double labeled neurons (yellow) (F). Scale bars = (A–C) 50 μ m; (D–F) 100 μ m; (G–O) 50 μ m. Photomicrographs J–L are acquired by confocal microscope

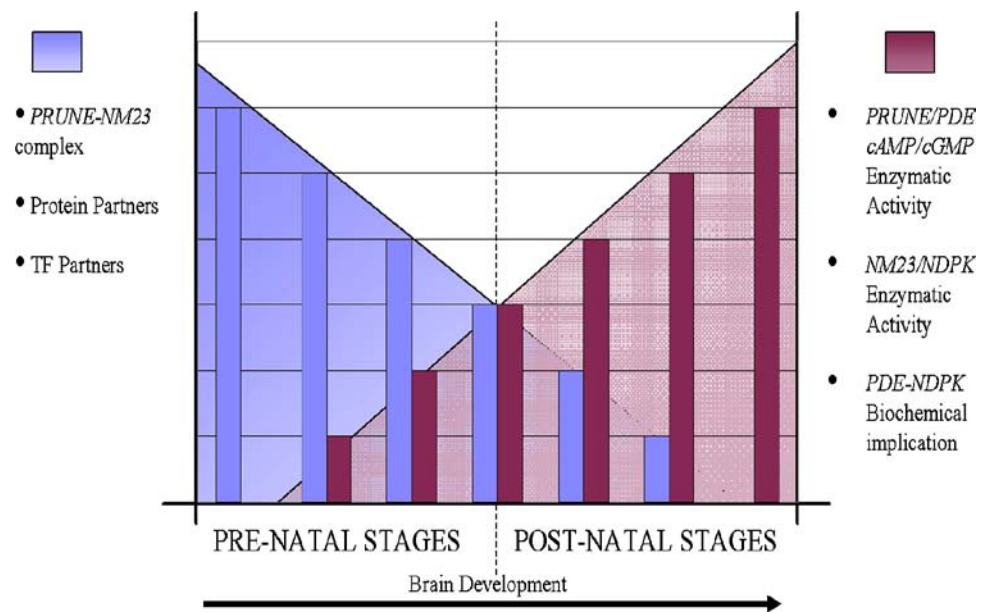


surface, in both of the layers of the forebrain mantle that retain differentiating neurons (Fig. 2C–F). It is interesting to note that the *PRUNE* and *NM23-M1* transcripts are expressed in all areas of the developing cerebellum from which the most important neuron population starts its differentiation processes (Fig. 5C–F). Both granular and Purkinje neuron precursors are abundantly labeled, suggesting a fundamental function of *PRUNE* and *NM23-H1* during the pro-

liferation, migration and differentiation processes of these cells.

The effects on cell motility and migration of the *NM23-H1* gene have already been demonstrated in several cancer cell types (Steege et al., 1988; Leone et al., 1991); moreover, *NM23-M1* has been shown to have an influence on neuronal proliferation and differentiation (Gervasi et al., 1996). According to the literature, these effects are not related to

Fig. 8 Integrated model of PRUNE and NM23 functions in the embryonic and adult brains. In the prenatal stages, we postulate that the role of *PRUNE* and *NM23* mainly involves PRUNE-NM23 complex formation, with protein partners and transcription factors (TF) of both genes regulating the brain developmental processes. In the adult, the enzymatic biochemical functions of PRUNE PDE-cAMP or -cGMP and of NM23 NDPK, and their mutual correlation, appear to take part in brain cognitive and somatic-sensory functions



NDPK enzyme activity. The second most important functions of *NM23-H1* are its anti-motility and anti-metastatic effects (Leone et al., 1993). In consideration of the negative regulation on the *NM23* anti-motility function of human *PRUNE* in breast cancer (D'Angelo et al., 2004), we now hypothesize that human *PRUNE* regulates the *NM23* pro-differentiation and anti-motility functions with the same strength in neuronal developmental processes. We reason that the different oligomeric species of the *NM23* genes could participate in a complex with *PRUNE* and other proteins in different developmental processes where the enzyme activity is not strictly required. Together with data already reported in the literature, our results show a distribution of *NM23-M1* and *PRUNE-M1* transcripts that is similar to that of the *m-Numb*, *Numbl* and *NOTCH1* genes in the embryonic cortex at E14.5 (Zhong et al., 1997). It is of note that during mouse cortical organogenesis, an asymmetric cell division is necessary to support the loss of cellular contacts from the basal cell layer before migration occurs towards the cortical plate layer, where it differentiates into post-mitotic neurons. As with *m-Numb*, *Numbl* and *NOTCH1*, *PRUNE* and *NM23* might be involved in both progenitor cell proliferation and neuronal differentiation in cortical neurogenesis processes. Additionally, an association of *NM23* with microtubules has been demonstrated in several studies, using biochemical methods and confocal laser scanning microscopy (Nickerson et al., 1984; Lombardi et al., 1995). These findings can be linked to the recent data of Garzia et al., 2006 (this issue). Indeed, a strong co-localization of human *PRUNE* with *F-ACTIN* was seen, and a physical interaction of human *PRUNE* with *paxillin*, *vinculin* and *GSK-3 β* was demonstrated in focal adhesions in several cell types including breast, thus postulating the association of *PRUNE*

with the microtubular architecture and dynamics in the cell (Kobayashi et al., 2006; Garzia et al., 2006 in this issue). These data could contribute to the elucidation of the molecular mechanisms by which *PRUNE* and *NM23* modulate the cell-shape processes involved in the development, proliferation, migration, differentiation and potentially in cell polarity of neuronal cells. Any defects in the above-described processes can cause several types of cortical developmental malformations, such as microgyria (OMIM 606854), heterotopia (OMIM 606854), lissencephaly (OMIM 607432), epilepsy (OMIM 607432) and inherited cerebellar disorders (Friedreich's ataxia, OMIM 229300); spinocerebellar ataxia, OMIM 164400). Whether the *PRUNE-NM23* combination and their regulation of expression during brain development is directly or indirectly involved in human brain genetic disorders is to date still an open question that will need further efforts, perhaps by using traditional linkage association analyses, because of their additional multifactorial genetic disease definition.

On the other hand, the expression of *PRUNE* and *NM23* at postnatal stages is more restricted than at embryonic stages; indeed, the two transcripts were detected only in a few specialized brain areas. Furthermore, strong expression of *PRUNE* and *NM23-M1* was detected in postnatal mouse cortical layers II and IV (Figs. 3 and 4); the cortical neurons of layer II are known to be the most important elements of the cortico-cortical integration network in the neocortex (Erchova et al., 2004). Moreover, it is known that sensory signal processing in cortical layer IV involves two major morphological classes of excitatory neurons: the spiny stellate and the pyramidal cells. These two cell types are integrated into intracortical networks and they have important roles in cortical signal processing (Schubert et al., 2003).

The expression of *PRUNE-M1* and *NM23-M1* in these layers suggests their involvement in somatosensory processing regulated by neurons of cortical layers II and IV, and a potential role of their complex in synaptic function and plasticity (Figs. 3 and 4). Their expression was also seen in other regions of the adult forebrain, including the basal ganglia of the striatum (Fig. 3). Synaptic transmission is believed to be regulated by vesicle trafficking; it has been shown that enzymatically active *NM23* is required for the synaptic vesicle internalization that requires the GTPase *dynamine* (Krishnan et al., 2001), and also that *NM23-M1* can bind *phocein*, a component of the complexes involved in critical steps of the vesicular trafficking machinery (Baillat et al., 2002). To date, how the *PRUNE-NM23* interaction is involved in the signaling pathways that regulate synaptic plasticity remains an interesting open question, and it is the object of further studies. It has been postulated that *PRUNE* can influence the enzyme activity of *NM23* by stabilization of its multimeric forms (D'Angelo et al., 2004) because the *K-pn* loop interaction is involved in the stabilization of the quaternary structure of *NM23* (Roymans et al., 2002). On the other hand, we can hypothesize a role in signaling pathways mainly because of the *PRUNE* PDE-cAMP enzyme activity. Activation of cAMP/protein kinase A (PKA) signaling may be necessary and sufficient for the induction of neuronal plasticity (Abel et al., 1997). Interesting, the cAMP/calcium response element (CRE) pathway has several properties that implicate it in memory formation in the hippocampus (Fortin et al., 2002). *PRUNE* and *NM23* expression in all areas of the adult mouse hippocampus allow us to suggest their involvement in the cAMP/CREB signaling that regulates memory pathway formation. Additionally, the PDE activity of *PRUNE* could explain its expression in the adult cerebellum. Many PDEs have been shown to be highly expressed in the cerebellum (*PDE5*, *PDE9* and *PDE7B*; Shimizu-Albergine et al., 2003; Reyes-Irisarri et al., 2005). In particular, *PDE5* has been shown to be involved in long-term depression (LTD), a decrease of synaptic transmission occurring between parallel fibers and Purkinje cells in the cerebellum. This last has been suggested as a mechanism of regulation of motor learning (Shimizu-Albergine et al., 2003). Our current hypothesis is that the *PRUNE* PDE-cAMP function is involved together with *NM23* in important cerebellar functions that are regulated by synaptic transmission.

We have also shown the expression of *PRUNE* and *NM23* in dopaminergic neurons of the substantia nigra. Neurodegeneration in this area causes neurodegenerative disorders such as Alzheimer's disease (OMIM 104300). Using proteomics techniques, which have been able to measure NDPK activity in human brain, an involvement of *NM23-H1* and *NM23-H2* in Alzheimer's disease has already been proposed (Kim et al., 2002). Considering that *PRUNE* binding might influence NDPK activity, we hypothesize a correlation of

the *PRUNE-NM23* complex with neurodegenerative disorders. These findings are thus of great interest, although they need further studies at this time.

We also suggest here an integrated model of the putative functions of the *PRUNE* and *NM23* complex in embryonic and adult brain (Fig. 8). At the embryonic stages of brain development, *PRUNE* and *NM23* functions do not appear to be related to their enzyme activities; instead, their functions are mainly due to their interactions or to their binding to other proteins involved in processes regulating brain development. In contrast, in adult brain, *PRUNE* and *NM23* functions might to be linked predominantly to their PDE and NDPK enzyme activities; several findings have suggested that these similar enzyme activities regulate synaptic transmission and signaling in the mammalian adult brain. Of course, the balance between these two potential functions can be altered and will be an issue of further studies, especially those involving *ad hoc* animal models. Nevertheless, the integrated biology of these two proteins remains to be deciphered, and it looks very promising in the framework of understanding brain development and morphology, and in adult cognitive and somatic CNS functions in human.

Acknowledgments This work was supported by an "AIRC-FIRC regionale, 2005" grant (M.Z.), a Medical Genetics PhD joint programme between TIGEM and Seconda Università di Medicina Napoli (P.C.), a Molecular Oncology and Pharmacology PhD programme (University of Ferrara, Italy) (N.M.), a FIRB-MIUR-RBAU01RW82 grant (M.Z.), and an EU BRECOSM-LSH-CT-503234 (M.Z.) FP6 grant. We additionally thank Dr. Nino Cozzolino and Dr. Enrico Gonzales (Ospedale Cardarelli, Centro di Biotecnologie), for animal housing and supports for mice embryos developments and characterization, OPEN, Associazione Oncologia Pediatrica e Neuroblastoma, (Salerno, Italy), and Fondazione Neuroblastoma Onlus (Genova, Italy).

Bibliography

- Abel T, Nguyen PV, Barad M, Deuel TAS, Kandel ER (1997) *Cell* 88:615–626
- Amendola R, Martinez R, Negroni A, Venturelli D, Tanno B, Calabretta B, Raschella G (1997) *J Natl Cancer Inst* 89:1300–1310
- Amendola R, Martinez R, Negroni A, Venturelli D, Tanno B, Calabretta B, Raschella G (2001) *Med Pediatr Oncol* 36:93–96
- Amrein L, Barraud P, Daniel J-Y, Pérel Y, Landry M (2005) *Cell Tissue Res* 322(3):365–378
- Baillat G, Gaillard S, Castets F, Monneron A (2002) *J Biol Chem* 277(21):18961–18966. Epub 2002 Feb 28
- Beadle GW, Ephrussi B (1936) *Genetics* 21:225–247
- Biggs J, Tripoulas N, Hersperger E, Dearolf C, Shearn A (1988) *Genes Dev* 2:1333–1343
- Colvin JS, Feldman B, Nadeau JH, Goldfarb M, Ornitz DM (1999) *Dev Dyn* 216(1):72–88
- Dabernat S, Larou M, Masse K, Dobremez E, Landry M, Mathieu C, Daniel JY (1999) *Gene* 236(2):221–230
- Dabernat S, Larou M, Masse K, Hokfelt T, Mayer G., Daniel JY, Landry M (1999) *Brain Res Mol Brain Res* 63(2):351–365

- D'Angelo A, Garzia L, Andre A, Carotenuto P, Aglio V, Guardiola O, Arrigoni G, Cossu A, Palmieri G, Aravind L, Zollo M (2004) *Cancer Cell* 5(2):137–149
- Dearolf C, Hersperger E, Shearn, A (1988a) *Develop Biol* 129:159–168
- Dearolf C, Tripoulas N, Biggs J, Shearn A (1988b) *Develop Biol* 129:169–178
- Dirk S, Kötter R, Zilles K, Luhmann HJ, Staiger JF (2003) *The J Neurosci* 23(7):2961
- Feijen A, Goumans MJ, van den Eijnden-van Raaij AJ (1994) *Development* 120(12):3621–3637
- Fortin NJ, Agster KL, Eichenbaum HB (2002) *Nat Neurosci* 5(5):458–462
- Forus A, D'Angelo A, Henriksen J, Merla G, Maelandsmo GM, Florenes VA, Olivieri S, Bjerkehagen B, Meza-Zepeda LA, del Vecchio Blanco F, Muller C, Sanvito F, Kononen J, Nesland JM, Fodstad O, Reymond A, Kallioniemi OP, Arrigoni G, Ballabio A, Myklebost O, Zollo M (2001) *Oncogene* 20(47):6881–6890
- Frolov MV, Zverlov VV, Alatorsev VE (1994) *Molec gen Genet* 242:478–483
- Garzia L, Roma C, Tata N, Pagnozzi D, Pucci P, Zollo M (2006) *J Bioenerg Biomembr*. (in this issue)
- Gervasi F, Capozza F, Bruno T, Fanciulli M, Lombardi D (1998) *DNA Cell Biol* 17(12):1047–1055
- Gervasi F, D'Agnano I, Vossio F, Zupi G, Sacchi A, Lombardi D (1996) *Cell Growth Differ* 7:1689–1695
- Hackstein JH (1992) *Eur J Cell Biol* 58(2):429–444
- Hartsough MT, Steeg PS (2000) *J Bioenerg Biomembr* 32:301–308
- Hsu S, Huang F, Wang L, Banerjee S, Winawer S, Friedman E (1994) *Cell Growth Differ* 5(9):909–917
- Kim SH, Fountoulakis M, Cairns NJ, Lubec G (2002) *Biophys Res Commun* 296(4):970–975
- Kobayashi T, Hino S, Oue N, Asahara T, Zollo M, Yasui W, Kikuchi A (2006) *Molecular Cell Biology*, 2006 in press
- Krishnan KS, Rikhy R, Rao S, Shivalkar M, Mosko M, Narayanan R, Etter P, Estes PS, Ramaswami M (2001) *Neuron* 30(1):197–210
- Lacombe ML, Milon L, Munier A, Mehus JG, Lambeth DO (2000) *J Bioenerg Biomembr* 32(3) 2000
- Lakso M, Steeg PS, Westphal H (1992) *Cell Growth Differ* 3(12):873–879
- Lascu I, Chaffotte A, Limbourg-Bouchon B, Veron M (1992) *J Biol Chem* 267:12775–12781
- Leone A, Flatow U, King CR, Sandeen MA, Margulies IMK, Liotta LA, Steeg PS (1991a) *Cell* 65:25–35
- Leone A, Flatow U, VanHoutte K, Steeg PS (1993a) *Oncogene* 8:2325–2333
- Lim S, Lee HY, Lee H (1998) *Cancer Lett* 133(2):143–149
- Lombardi D, Sacchi A, D'Agostino G, Tibursi G (1995) *Exp Cell Res* 217(2):267–271
- Lombardi D, Lacombe ML, Paggi MG (2000) *J Cell Physiol* 182:144–149
- Mesnilidrey S, Agou F, Karlsson A, Bonne DD, Veron M (1998) *J Biol Chem* 273(8):4436–4442
- Nickerson JA, Wells WW (1984) *J Biol Chem* 259(18):11297–11304
- Ohkura N, Kishi M, Tsukada T, Yamaguchi K (2001) *Biochem Biophys Res Commun* 282(5):1206–1210
- Orevi N, Falk R (1974) *Arch Genet (Zur)*. 47(3):172–183
- Otero AS (2000) *J Bioenerg Biomembr* 32:269–275
- Paravicini G, Steinmayr M, Andre E, Becker-Andre M (1996) *Biochem Biophys Res Commun* 227(1):82–87
- Reyes-Irisarri E, Perez-Torres S, Mengod G (2005) *Neuroscience* 132(4):1173–1185
- Reymond A, Volorio S, Merla G, Al-Maghteh M, Zuffardi O, Bulfone A, Ballabio A, Zollo M (1999) *Oncogene* 18(51):7244–7252
- Rosengard A, Krutzsch H, Shearn A, Biggs J, Barker E, Margulies I, Richter-King C, Liotta L, Steeg P (1989) *Nature (London)* 342:177–180
- Roymans D, Willems R, Vissenberg K, De Jonghe C, Grobben B, Claes P, Lascu I, Van Bockstaele D, Verbelen JP, Van Broeckhoven C, Slegers H (2000) *Exp Cell Res* 25:261(1):127–138
- Shimizu-Albergine M, Rybalkin SD, Rybalkina IG, Feil R, Wolfsgruber W, Hofmann F, Beavo JA (2003) *J Neurosci* 23(16):6452–6459
- Steeg PS, Bevilacqua G, Kopper L, Thorgeirsson UP, Talmadge JE, Liotta LA, Sobel ME J (1988) *Natl Cancer Inst* 80(3):200–204
- Sturtevant AH (1956) *Genetics* 41:118–123
- Subramanian C, Cotter MA 2nd, Robertson ES (2001) *Nat Med* 7(3):350–355
- Suzuki E, Ota T, Tsukuda K, Okita A, Matsuoka K, Murakami M, Doihara H, Shimizu N (2004) *Int J Cancer* 108(2):207–211
- Teng DH, Bender LB, Engele CM, Tsobuta S, Ven-katesh T (1991a) *Genetics* 128:373–380
- Timmons L, Shearn A (1996) *Genetics* 144:1589–1600
- Timmons L, Xu J, Hersperger G, Deng X-F, Tharakan M, Shearn A (1995) *J Biol Chem* 270: 23021–23030
- Zhong W, Jiang MM, Weinmaster G, Jan LY, Jan YN (1997) *Development* 124(10):1887–1897